Taylor & Francis
Taylor & Francis Group

Natural Product Research
Formerly Natural Product Letters

ISSN: 1478-6419 (Print) 1478-6427 (Online) Journal homepage: https://www.tandfonline.com/loi/gnpl20

Synthesis, α-Glucosidase inhibition and molecular docking studies of tyrosol derivatives

Luyun Zhang, Qian Xu, Junyi Zhu, Guangqing Xia & Hao Zang

To cite this article: Luyun Zhang, Qian Xu, Junyi Zhu, Guangqing Xia & Hao Zang (2019): Synthesis, α-Glucosidase inhibition and molecular docking studies of tyrosol derivatives, Natural Product Research

To link to this article: https://doi.org/10.1080/14786419.2019.1628750

NATURAL PRODUCT RESEARCH
https://doi.org/10.1080/14786419.2019.1628750

Synthesis, α-Glucosidase inhibition and molecular docking studies of tyrosol derivatives

Luyun Zhang[a,b], Qian Xu[a,c], Junyi Zhu[a], Guangqing Xia[a,b] and Hao Zang[a,c]

[a]School of Pharmacy and Medicine, Green Medicinal Chemistry Laboratory, Tonghua Normal University, Tonghua, China; [b]Changchun University of Chinese Medicine, Jilin Ginseng Academy, Changchun, China; [c]College of Medicine, Yanbian University, Yanji, China

ABSTRACT

To find a potent α-glucosidase inhibitor, 24 tyrosol derivatives with different substituents located at the *meta*, *ortho*, or *para* position of the phenyl group have been synthesised via the Mitsunobu reaction, characterised by ^{1}H NMR, ^{13}C NMR, ESI-MS and IR and evaluated for inhibition. The derivatives possessed varying degrees of *in vitro* inhibitory activity against α-glucosidase and a relationship between the structure and activity was subsequently established for all compounds. Two of these compounds with substituents at the *para* position showed significant inhibitory effects surpassing that of the control standard acarbose. Molecular docking studies performed to better understand the binding interactions between the enzyme and the two most active compounds showed substantial binding within the active site of α-glucosidase. Taken together, these results indicate that the position of the substituent plays a crucial role in this inhibition and may facilitate the development of new α-glucosidase inhibitors.

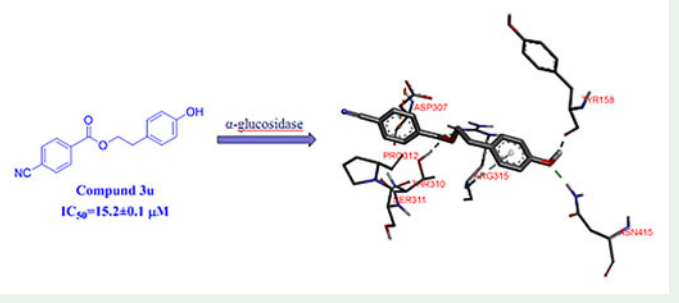

ARTICLE HISTORY
Received 29 March 2019
Accepted 31 May 2019

KEYWORDS
tyrosol; synthesis; α-glucosidase; structure activity relationship; molecular docking

1. Introduction

Diabetes is a complicated chronic metabolic disorder of which there are two clinical types. Type I diabetes is caused by an insufficient insulin secretion, whereas Type II

CONTACT Hao Zang zanghao_1984@163.com; Junyi Zhu swx0527@163.com;
Guangqing Xia qingguangx@163.com

Supplemental data for this article can be accessed at http://dx.doi.org/10.1080/14786419.2019.1628750.

diabetes is caused by an insufficient insulin utilisation (Wang et al. 2016). Postprandial hyperglycaemia is a major feature in diabetes and causes many complications, including kidney disease, retinopathy and cardiovascular disease (Han et al. 2017). One of the most effective approaches to reducing postprandial blood glucose is to inhibit the activity of carbohydrate hydrolases, especially α-glucosidase in the intestinal epithelial cells (Schmidt et al. 2014). α-Glucosidase hydrolyses α-1,4 glycosidic bonds to release α-glucose, which is the final step in carbohydrate digestion (Shimba et al. 2009; Motabar et al. 2009). Therefore, α-glucosidase inhibitors can effectively control postprandial hyperglycaemia. Some α-glucosidase inhibitors, such as acarbose and voglibose, have been clinically applied to treat diabetes. However, there are increasingly more reports on their side effects, which include abdominal pain, diarrhoea and other gastrointestinal diseases (Wei et al. 2017; Peng et al. 2016). Therefore, it is urgent to find effective α-glucosidase inhibitors with fewer side effects.

Tyrosol is one of the major natural phenolic antioxidants contained in olive oil (Servili et al. 2009) and has been reported to possess various physiological benefits because of its potent antioxidant activity (Giovannini et al. 1999).

Recent studies have suggested that tyrosol possesses antigenotoxic activity and may prevent apoptosis in keratinocytes (Salucci et al. 2015). Other studies indicate that it may play a role in preventing Alzheimer's disease and Parkinson's disease by antagonizing the β-amyloids and inhibiting apoptosis of dopaminergic neurons (St-Laurent-Thibault et al. 2011; Dewapriya et al. 2013). In addition, there are claims that tyrosol can effectively increase longevity (Canuelo et al. 2012), reduce the risk of heart disease (Sun et al. 2015), and prevent cancer (Ahn et al. 2008). Tyrosol has been shown to exhibit α-glucosidase inhibitory activity (Kwon et al. 2006), and plays a role in the regulation of key enzymes in carbohydrate metabolism (Chandramohan et al. 2015; Chandramohan et al. 2017). Thus, tyrosol may be a promising candidate with the potential to facilitate the prevention and treatment of diabetes.

The structural modification of tyrosol is a research area of growing interest in the field of medicinal chemistry. In recent studies, tyrosol glucuronates have been prepared as antitrypanosomal and antileishmanial agents (Belmonte-Reche et al. 2016). Tyrosyl gallate has been prepared as potent melanin formation inhibitors (Lee et al. 2007). Other studies have focused on the synthesis of tyrosol ethers and esters and evaluating their antioxidant activities (Madrona et al. 2011; Zang et al. 2018; Zhou et al. 2017). In addition, tyrosol esters have been synthesised to investigate its role in the control of metastatic breast cancer (Busnena et al. 2013). To our knowledge, there have not been any studies on the hypoglycemic effect of tyrosol derivatives. Thus, we report herein the design and synthesis of tyrosol derivatives, and the characterisation of their α-glucosidase inhibitory activities in order to find highly active compounds.

2. Results and discussion

2.1. Chemistry

The 24 derivatives **3a**-**3x** were synthesised from tyrosol via the Mitsunobu reaction with substituted benzoic acid in tetrahydrofuran (THF) for 48 h to obtain overall high yields of the target compounds. the synthetic routes are outlined in Scheme 1.

2.2. Biological activity

The inhibitory activity of compounds **3a**-**3x** against α-glucosidase was then carried out. The results summarized in Table 1. In addition to compound **3m**, **3o**, **3r** and **3s**, other compounds showed a variable degree of α-glucosidase inhibition with IC_{50} values ranging between 15.2 and 730.5 μM in comparison with the positive control acarbose, which had an IC_{50} value of 60.9 μM. The structure and activity relationship was investigated by adding different substituents to the phenyl group.

Compounds **3u** displayed the most potent inhibitory activity among the series. The greater potential shown by this compound might be due to the electron-withdrawing cyano group. The most active compound **3u** (IC_{50}=15.2 μM), a *para*-cyano substituted derivative, was found to be superior in comparison with the compound **3s**(IC_{50}>800 μM) and **3t** (IC_{50}=394.9 μM) containing *ortho*-cyano and *meta*-cyano substituents, respectively. These results indicate that the position of the substituent plays a crucial role in this inhibition.

Table 1. α-Glucosidase inhibitory activity of compounds 3a-3x.

Compd.	Structure	IC_{50} (μM)	Compd.	Structure	IC_{50} (μM)
3a	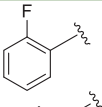	730.5 ± 9.3	**3m**	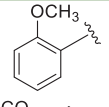	>800
3b	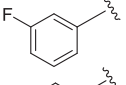	619.1 ± 7.6	**3n**	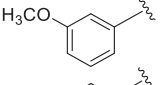	450.8 ± 3.8
3c	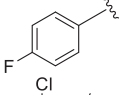	594.3 ± 5.7	**3o**	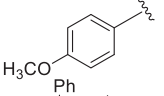	>800
3d	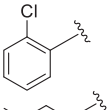	309.2 ± 4.0	**3p**	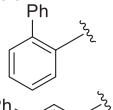	92.8 ± 0.5
3e	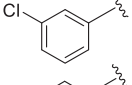	168.0 ± 2.3	**3q**	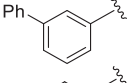	67.2 ± 0.8
3f	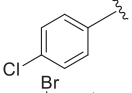	161.8 ± 2.1	**3r**	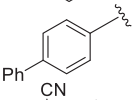	>800
3g	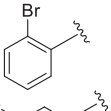	272.7 ± 1.9	**3s**	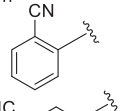	>800
3h	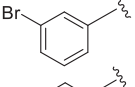	153.9 ± 1.5	**3t**	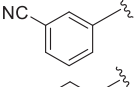	394.9 ± 3.4
3i	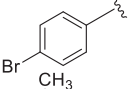	132.6 ± 1.3	**3u**	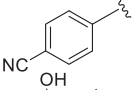	15.2 ± 0.1
3j	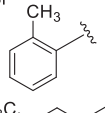	375.8 ± 2.5	**3v**	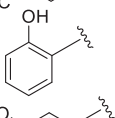	349.1 ± 2.4
3k	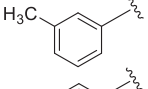	388.4 ± 2.1	**3w**	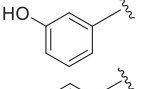	137.0 ± 0.9
3l	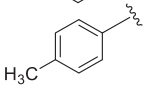	401.7 ± 2.1	**3x**	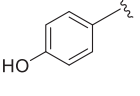	41.2 ± 0.2
Acarbose		60.9 ± 1.0			

A comparison of compound **3x** (IC_{50} = 41.2 μM) with **3v** (IC_{50} = 349.1 μM) and **3w** (IC_{50} =1 37.0 μM) shows that although these three derivatives have a hydroxyl group on the phenyl ring, the position of the hydroxyl group is different in each and their inhibitory activities vary. This confirms that the difference in the substituent position affects the inhibitory potentials of the compounds. Compounds having the hydroxyl substituent at the *para* position were able to efficiently inhibit α-glucosidase.

For compounds **3a**-**3c** with fluoro substituents at the *ortho*, *meta*, and *para* positions of the phenyl ring, respectively, the inhibitory potential was lowest for the *ortho*-fluoro substituent (**3a**) and highest for the *para*-fluoro substituent (**3c**). This further supports that the position of the substituent is important in this inhibition. A similar pattern was also observed for other derivatives in this series.

For electron-withdrawing and electron-donating groups on the phenyl ring, we observed that the location of the substituent influenced the inhibitory properties of the tyrosol derivatives. The compounds with electron-withdrawing substituents at the *para* position were more active than their *meta* and *ortho* counterparts. In contrast, the compounds containing electron-donating substituents at the *meta* position were found to be more active than their *para* and *ortho* counterparts. To understand the binding interaction of the most active derivatives, molecular docking studies were performed.

2.4. Docking results

The molecular modelling simulation software AutoDock was used for the protein-ligand interaction study. The compound **3u** and **3x**, along with the control compound acarbose, were docked. Our analysis showed that the active molecules of the tyrosol derivatives displayed substantial binding within the active site of α-glucosidase. Overall, the tyrosol derivatives with either a cyano or hydroxyl group at the *para* position on the phenyl ring showed good activity.

The most active derivative among the series is compound **3u** and is shown in Figure 1. The hydroxyl group of the tyrosol formed H-bond with Tyr158 and Asn415, whilst the carbonyl group of the *para*-cyanobenzoic acid formed H-bond with Arg315 and Thr310; these were the main interactions between **3u** and α-glucosidase. Ser311 formed an amide-π stacking with the phenyl ring of the *para*-cyanobenzoic acid.

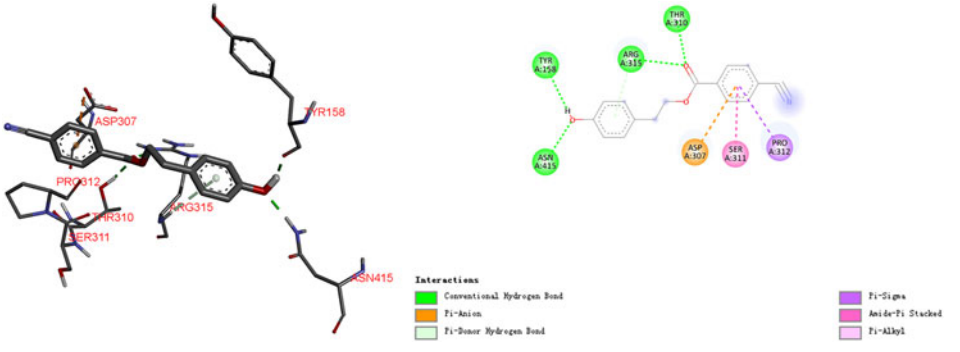

Figure 1. Compound **3u** was docked to the binding pocket of the α-glucosidase.

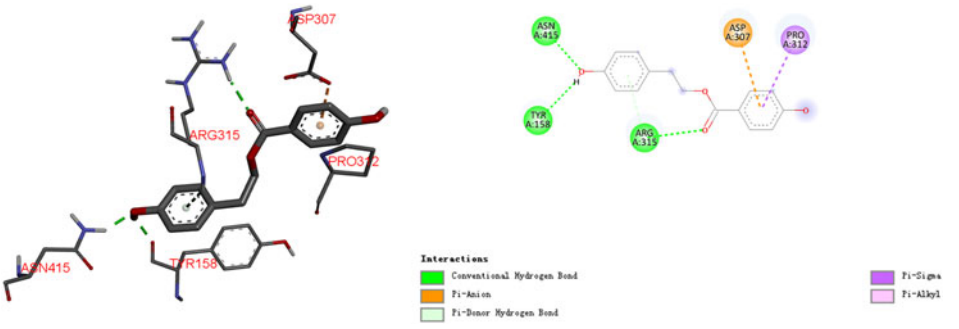

Figure 2. Compound **3x** was docked to the binding pocket of the α-glucosidase.

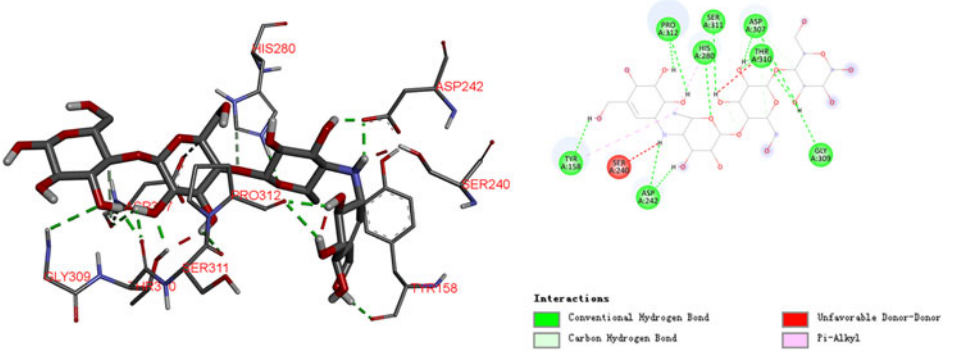

Figure 3. Acarbose was docked to the binding pocket of the α-glucosidase.

Additionally, the π-cation interactions and π-σ interactions were observed between the phenyl ring of the *para*-cyanobenzoic acid and the residues Asp307 and Pro312.

The second most active compound is compound **3x** and is shown in Figure 2. Similar to **3u**, the docking studies showed that the hydroxyl group of the tyrosol in **3x** formed H-bond with Tyr158 and Asn415, whilst the carbonyl group of the *para*-cyanobenzoic acid formed a H-bond with Arg315. For this derivative, the π-cation interactions and π-σ interactions were also observed between the phenyl ring of the *para*-cyanobenzoic acid and the residue Asp307 and Pro312.

A molecular docking study of the standard drug acarbose with α-glucosidase was also performed (Figure 3). The docking studies showed that the hydroxyl group of acarbose formed H-bond with Tyr158, Asp242, Pro312, His280, Ser311, Asp307, Thr310 and Gly309. Compound **3u** was the most active compound, followed by **3x** and their free binding energies were calculated to be −7.08 kcal/mol and -6.02 kcal/mol, respectively, which are lower than acarbose (−5.67 kcal/mol).

Taken together, the α-glucosidase inhibition results and molecular interaction studies clearly suggest that the cyano group and hydroxyl group attached to the *para* position of the phenyl ring from the tyrosol derivatives are responsible for influencing the inhibitory activity. The presence of a hydrophilic group on the phenyl ring was accountable for the improvement of activity, which provided valuable information for the design of inhibitory compounds.

3. Experimental

3.1. General information

Yeast α-Glucosidase (EC 3.2.1.20) was purchased from the supplier (Sigma-Aldrich). Acarbose 98% from Ark Pharm. p-Nitrophenyl-α-D-glucopyranoside (pNPG, 99%) from Acros. Tyrosol, 98%, Triphenylphosphine (TPP, 98%), Diisopropyl azodicarboxylate (DIAD, 97%), dry THF, 99.5% were purchased from the supplier (Energy Chemical). EtOAc, 99.5%, Methanol, 99.5% were used as received from the supplier (Sinopharm Chemical).

Column chromatography was carried out on silica gel (200-300 mesh). Thin layer chromatography (TLC) was performed using silica gel 60 F_{254} plates. ^{1}H NMR and ^{13}C NMR spectra were measured on an AV-600 Spectrometer (Bruker, Germany) using tetramethylsilane as an internal standard. Electrospray ionization mass spectrometry (ESI-MS) were performed on an Aglient 6520 Q-TOF (Agilent, USA) in positive ionization mode. Epoch microplate spectrophotometer (BioTek, USA). Melting points were determined in open capillary tubes and the temperature was uncorrected.

3.2. Synthesis

A general experimental procedure for the synthesis of compounds (**3a-3x**)

The target compounds were synthesised as outlined in our previously published work (Zang et al. 2018). Tyrosol **1** (0.4 mmol, 1.0 equiv), organic acids **2** (0.4 mmol, 1.0 equiv) and TPP (0.4 mmol, 1.0 equiv) were placed in a dry standard Schlenk tube under N_2. Dry THF (1.0 mL) was added, followed by the addition of DIAD (0.4 mmol, 1.0 equiv) at 0 °C. The reaction mixture was stirred at room temperature for 48 h, and the reaction was monitored with thin-layer chromatography. The crude reaction mixture was purified by flash silica gel column chromatography (petroleum ether: ethyl acetate = 4:1) to obtain the corresponding product.

3.3. α-Glucosidase inhibition assay

α-Glucosidase was assayed according to the method with slight modifications (Yuan et al. 2012). Each sample in DMSO solution(20 μL) (from 0.1 to 10 mM) was added to 100 μL of α-Glucosidase solution (pH 6.9, 0.1 U/mL, in 0.1 M phosphate buffer). The reaction mixtures were incubated at 25 °C for 10 min. Then, 50 μL pNPG solution (pH 6.9, 5 mM, in 0.1 M phosphate buffer) was added to each well, the reaction mixtures were incubated at 25 °C for 5 min. Before and after incubation, the absorbance was recorded at 405 nm on a microplate spectrophotometer (BioTek). Acarbose was used as a positive reference. The α-Glucosidase inhibition activity was expressed as % inhibition and was calculated as follows:

$$\%inhibition = \left(1 - \frac{\Delta A_{sample}}{\Delta A_{control}}\right) \times 100\%$$

3.4. Statistical analysis

All the experiments were carried out in triplicate and the data were analyzed using SPSS software (Version 22.0) and Origin software (Version 8.0).

3.5. Molecular docking studies

To investigate the binding modes of compound **3u** and **3x**, a docking simulation was performed targeting the crystal structure of α-glucosidase. Because the crystal structure for α-glucosidase from *Saccharomyces cerevisiae* (*S. cerevisiae*) is still not available, a docking study was conducted using a homology model for α-glucosidase. Preliminary results on the sequence analysis of α-glucosidase from *S. cerevisiae* showed that the most suitable template for homology modelling is isomaltase (EC 3.2.1.10, oligo-1,6-glucosidase, MALX3) (protein data bank (PDB) ID: 3A4A) from baker's yeast. It shares 71% identity and 84% similarity with the target enzyme, α-glucosidase from *S. cerevisiae*. The crystal structure was retrieved from the PDB, and the α-glycosidase was pre-docked using the Autodock software. The **3D** structures of **3u** and **3x** were built with ChemBioDraw Ultra 14.0 and ChemBio3D Ultra 14.0, and then converted to PDBQT coordinates using AutoDockTools 1.5.6. In AutoGrid, maps were calculated for each atom type in the ligand with a 0.375 Å spacing between the grid points and the centre of the grid box was placed at x = 12.583, y = −7.896, z = 12.519. The dimensions size was set at 40 Å × 40 Å × 40 Å. Flexible ligand dockings were accomplished for the selected compounds. Each docked system was carried out by 50 runs of the AutoDock search by the Lamarckian genetic algorithm. The best positions of the selected compounds were chosen by analysing the interactions between the enzyme and inhibitors. The best-scoring positions, as judged by the docking score, were then selected and visually analysed using Discovery Studio Client 2017.

4. Conclusion

In summary, a series of tyrosol derivatives have been synthesised and screened for α-glucosidase inhibitory activity. Compound **3u** (IC_{50}=15.2 μM) and **3x** (IC_{50}=41.2 μM) showed significant inhibitory effects, which surpassed that of the control standard acarbose (IC_{50}=60.9 μM). The structure and activity relationship was examined by designing tyrosol derivatives with various substituents at different positions on the phenyl group, and evaluating how the position affected the inhibitory properties of the tyrosol derivatives. The binding interactions of the most active compounds were confirmed through molecular docking studies, which showed substantial binding within the active site of α-glucosidase. The compounds synthesised in this study have demonstrated that the position of the substituent plays a crucial role in affecting the inhibition activity, and may be useful for the development of new α-glucosidase inhibitors.

Acknowledgement

We thank Rosalie Tran, PhD, from Liwen Bianji, Edanz Editing China (www.liwenbianji.cn/ac), for editing the English text of a draft of this manuscript.

Disclosure statement

The authors declare no conflict of interest.

Funding

This work is supported by the Science and Technology Development Funds of Jilin Province (No. 20160520044JH) and the Science and Technology Projects of Administration of Traditional Chinese Medicine of Jilin Province (No. 2019145).

References

Ahn EY, Jiang Y, Zhang Y, Son EM, You S, Kang SW, Park JS, Jung JH, Lee BJ, Kim DK. 2008. Cytotoxicity of p-tyrosol and its derivatives may correlate with the inhibition of DNA replication initiation. Oncol Rep. 19(2):527–534.

Belmonte-Reche E, Martinez-Garcia M, Penalver P, Gomez-Perez V, Lucas R, Gamarro F, Perez-Victoria JM, Morales JC. 2016. Tyrosol and hydroxytyrosol derivatives as antitrypanosomal and antileishmanial agents. Eur J Med Chem. 119:132–140.

Busnena BA, Foudah AI, Melancon T, El Sayed KA. 2013. Olive secoiridoids and semisynthetic bioisostere analogues for the control of metastatic breast cancer. Bioorg Med Chem. 21(7): 2117–2127.

Canuelo A, Gilbert-Lopez B, Pacheco-Linan P, Martinez-Lara E, Siles E, Miranda-Vizuete A. 2012. Tyrosol, a main phenol present in extra virgin olive oil, increases lifespan and stress resistance in *Caenorhabditis elegans*. Mech Ageing Dev. 133(8):563–574.

Chandramohan R, Pari L, Rathinam A, Sheikh BA. 2015. Tyrosol, a phenolic compound, ameliorates hyperglycemia by regulating key enzymes of carbohydrate metabolism in streptozotocin induced diabetic rats. Chem Biol Interact. 229:44–54.

Chandramohan R, Saravanan S, Pari L. 2017. Beneficial effects of tyrosol on altered glycoprotein components in streptozotocin-induced diabetic rats. Pharm Biol. 55(1):1631–1637.

Dewapriya P, Himaya SW, Li YX, Kim SK. 2013. Tyrosol exerts a protective effect against dopaminergic neuronal cell death in *in vitro* model of Parkinson's disease. Food Chem. 141(2): 1147–1157.

Giovannini C, Straface E, Modesti D, Coni E, Cantafora A, De Vincenzi M, Malorni W, Masella R. 1999. Tyrosol, the major olive oil biophenol, protects against oxidized-LDL-induced injury in Caco-2 cells. J Nutr. 129(7):1269–1277.

Han L, Fang C, Zhu R, Peng Q, Li D, Wang M. 2017. Inhibitory effect of phloretin on α-glucosidase: Kinetics, interaction mechanism and molecular docking. Int J Biol Macromol. 95: 520–527.

Kwon YI, Jang HD, Shetty K. 2006. Evaluation of *Rhodiola crenulata* and *Rhodiola rosea* for management of type II diabetes and hypertension. Asia Pac J Clin Nutr. 15(3):425–432.

Lee CW, Son EM, Kim HS, Xu P, Batmunkh T, Lee BJ, Koo KA. 2007. Synthetic tyrosyl gallate derivatives as potent melanin formation inhibitors. Bioorg Med Chem Lett. 17(19):5462–5464.

Madrona A, Pereira-Caro G, Bravo L, Mateos R, Espartero JL. 2011. Preparation and antioxidant activity of tyrosyl and homovanillyl ethers. Food Chem. 129(3):1169–1178.

Motabar O, Shi ZD, Goldin E, Liu K, Southall N, Sidransky E, Austin CP, Griffiths GL, Zheng W. 2009. A new resorufin-based α-glucosidase assay for high throughput screening. Anal Biochem. 390(1):79–84.

Peng X, Zhang G, Liao Y, Gong D. 2016. Inhibitory kinetics and mechanism of kaempferol on α-glucosidase. Food Chem. 190:207–215.

Salucci S, Burattini S, Battistelli M, Buontempo F, Canonico B, Martelli AM, Papa S, Falcieri E. 2015. Tyrosol prevents apoptosis in irradiated keratinocytes. J Dermatol Sci. 80(1):61–68.

Schmidt JS, Nyberg NT, Staerk D. 2014. Assessment of constituents in Allium by multivariate data analysis, high-resolution α-glucosidase inhibition assay and HPLC-SPE-NMR. Food Chem. 161:192–198.

Servili M, Esposto S, Fabiani R, Urbani S, Taticchi A, Mariucci F, Selvaggini R, Montedoro GF. 2009. Phenolic compounds in olive oil: antioxidant, health and organoleptic activities according to their chemical structure. Inflammopharmacol. 17(2):76–84.

Shimba N, Shinagawa M, Hoshino W, Yamaguchi H, Yamada N, Suzuki E. 2009. Monitoring the hydrolysis and transglycosylation activity of alpha-glucosidase from *Aspergillus niger* by nuclear magnetic resonance spectroscopy and mass spectrometry. Anal Biochem. 393(1): 23–28.

St-Laurent-Thibault C, Arseneault M, Longpre F, Ramassamy C. 2011. Tyrosol and hydroxytyrosol, two main components of olive oil, protect N2a cells against amyloid-β-induced toxicity. Involvement of the NF-κB signaling. Curr Alzheimer Res. 8(5):543–551.

Sun L, Fan H, Yang L, Shi L, Liu Y. 2015. Tyrosol prevents ischemia/reperfusion-induced cardiac injury in H9c2 cells: involvement of ROS, Hsp70, JNK and ERK, and apoptosis. Molecules. 20(3):3758–3775.

Wang G, Wang J, He D, Li X, Li J, Peng Z. 2016. Synthesis and biological evaluation of novel 1,2,4-triazine derivatives bearing carbazole moiety as potent α-glucosidase inhibitors. Bioorg Med Chem Lett. 26(12):2806–2809.

Wei M, Chai WM, Yang Q, Wang R, Peng Y. 2017. Novel insights into the inhibitory effect and mechanism of proanthocyanidins from *pyracantha fortuneana* fruit on α-Glucosidase. J Food Sci. 82(10):2260–2268.

Yuan T, Wan C, Liu K, Seeram NP. 2012. New maplexins F-I and phenolic glycosides from red maple (*Acer rubrum*) bark. Tetrahedron. 68(4):959–964.

Zang H, Shen P, Wang EP, Xu Q, Zhang LY, Xia GQ, Zhu JY, Zhang H, Yang XH. 2018. Synthesis and biological activity of tyrosol ester derivatives. Chem J Chinese Universities. 39:64–70.

Zhou D, Sun Y, Shahidi F. 2017. Preparation and antioxidant activity of tyrosol and hydroxytyrosol esters. J Funct Foods. 37:66–73.